Biosensors and Bioelectronics ■ (■■■■) ■■■–■■■

Contents lists available at ScienceDirect

Biosensors and Bioelectronics

journal homepage: www.elsevier.com/locate/bios

Detection of CTX-II in serum and urine to diagnose osteoarthritis by using a fluoro-microbeads guiding chip

Yoo Min Park [a], Su Jin Kim [a], Ki Jung Lee [b], Sang Sik Yang [b], Byoung-Hyun Min [c], Hyun C. Yoon [a,*]

[a] Department of Molecular Science and Technology, Ajou University, Suwon 443749, South Korea
[b] Department of Electrical and Computer Engineering, Ajou University, South Korea
[c] Department of Orthopedic Surgery, School of Medicine, Ajou University, South Korea

ARTICLE INFO

Article history:
Received 23 May 2014
Received in revised form
4 August 2014
Accepted 11 August 2014

Keywords:
Osteoarthritis
sCTX-II
uCTX-II
Immunosensing
Fluoro-microbeads

ABSTRACT

This study reports a new strategy for simultaneous detection of the C-telopeptide fragments of type II collagen (CTX-II) as a biomarker of osteoarthritis (OA) using a fluoro-microbeads guiding chip. As osteoarthritis progresses, the joint components including matrix and cartilage are degraded by proteases. The degraded products such as CTX-II are released into the serum and urine, and the CTX-II concentration in body fluids reflects OA progression. Because the CTX-II has heterogeneous epitope structure in serum (sCTX-II; homodimers) and urine (uCTX-II; monomers or variant monomers), a multiple-sensing device enabling both sandwich and competitive-type immunoassays is required. For multiple assessments of serum and urinary CTX-II, we designed a fluoro-microbeads guiding chip (FMGC) containing multiple sensing areas and connecting channels. Using the approach, the sandwich (sCTX-II) and competition (uCTX-II) assays could be simultaneously performed on a single chip. We designed a fluidic control device enabling selective control of the open–close function of FMGC channels. The immune-specific signal was quantitatively analyzed by counting the number of fluorescent microbeads from the registered images. The results from the developed FMGC assay showed high correlation with those obtained in ELISA. The completion time of the FMGC assay was 24-fold and 3.5-fold shorter than the ELISA for urinary and serum CTX-II. Taken together, it enabled the simultaneous detection of both sCTX-II and uCTX-II. This FMGC-based assay would be a promising tool for monitoring of osteoarthritis.

© 2014 Elsevier B.V. All rights reserved.

1. Introduction

Extensive studies employing biomarker-based analytical techniques have been carried out in industrial and academic fields because biomarker-based diagnosis is simpler and faster than tissue examination or image-based diagnostic methods (Wildi and Tamborrini, 2011). Numerous types of biomarkers exist in the body fluids of humans, and the biomarker levels reflect the state of diseases (Hanash et al., 2008; Giljohann and Mirkin, 2009). Therefore, sensitive and selective biosensors are helpful for early diagnosis and monitoring of diseases. OA, a common degenerative disease that leads to the loss of cartilage and destruction of joints, requires routine monitoring of its progression (Lohmander, 1997; Ding et al., 2005). Because OA progresses with aging, monitoring of the degenerative condition of joints is important to effectively care the disease (Roos et al., 1995; Zhang and Jordan, 2010). In the clinical field, the joint-space width is measured to assess the state of OA by using magnetic resonance imaging and radiography (Ding et al., 2005). However, reliable evaluation of the joint condition is time-consuming because alterations to the joint-space occur slowly (Rousseau and Delmas, 2007). To overcome the limitation, analytical techniques for cartilage-associated biochemical changes have been developed by monitoring biomarkers from the body fluids (Hong et al., 2012; Song et al., 2012).

OA biomarkers are enzymatic products or debris (peptide fragments) generated by the collagenase and proteases. As osteoarthritis progresses, the majority of biomarkers are accumulated in the synovial fluid and are then sequentially released into blood and urine. Therefore, the concentrations of OA biomarkers in body fluids increase as a function of the joint damage (Elsaid and Chichester, 2006; Kong et al., 2006). For this reason, we focused on the determination of OA biomarkers in various specimens. OA biomarkers such as proteases, joint substances, matrix proteins, and growth factors have been classified and ranked according to

* Corresponding author.
E-mail address: hcyoon@ajou.ac.kr (H.C. Yoon).

http://dx.doi.org/10.1016/j.bios.2014.08.016
0956-5663/© 2014 Elsevier B.V. All rights reserved.

the BIPEDS criteria (burden of disease, investigative, prognostic, efficacy of intervention, diagnostic, and safety of intervention) (Bauer et al., 2006; Garnero, 2007; Kraus et al., 2011). Among the candidate biomarkers, we specially focused on the CTX-II because this covers most of the BIPEDS criteria and ranked first (Birmingham et al., 2006; Lotz et al., 2013). Previous studies, for example, reported that the concentrations of CTX-II in urine and serum reflect the extent of cartilage damage (Garnero et al., 2002; Elsaid and Chichester, 2006; Tang et al., 2012). These studies employed a conventional ELISA for CTX-II analyses, requiring several hours for completion of the assay. Also, serum and urine samples should be properly diluted before each ELISA assays. To overcome these drawbacks, a new optical immunosensing system for simultaneous detection of CTX-II in serum and urine was proposed in this study.

The structure of serum CTX-II (sCTX-II) has not been thoroughly studied yet. In consideration of the CTX-II structure from synovial fluid having dimeric-hexapeptide epitope (EKGPDP) (Lohmander et al., 2003; Birmingham et al., 2006), we assumed that the sCTX-II would contain a similar cross-linked dimeric epitope. Therefore, a sandwich-type immunoassay was possible for the sCTX-II analysis. In contrast, urinary CTX-II (uCTX-II) which is transported through kidney may not have the intact cross-linked structure and even exhibits variant monomeric epitopes (Eyre et al., 2008). Based on the different structural properties of uCTX-II, a competition-type assay was conducted comparing to the sandwich-type assay for sCTX-II. The PEG-conjugated hexapeptide, PEG_4-EKGPDP, was used as a competition molecule for uCTX-II (Kim et al., 2013).

In order to determine CTX-II markers from two different sources simultaneously, we designed and fabricated a biosensing system containing immunoassay and fluidic control part. Previously, we reported the FMGC for multiple analyses of antigens at various concentrations in small-volume samples on a single chip (Song et al., 2011; Park et al., 2013). However, the solutions had to be applied individually to this device because it has separated channel arrangement. For simultaneous application of samples to a single immunosensing chip, we integrated four separate channels in a FMGC which could be controlled systematically. The sample solutions such as serum and urine could be applied to each individual channel on the FMGC by using a single injection channel. Additionally, the FMGC channels could be separately controlled for application of the heterogeneous sample on a single FMGC. To achieve this, we developed a fluidic control device (FCD), enabling a selective open–close action of each FMGC channels. Because the microfluidic channels were made of polydimethylsiloxane with high elasticity, the flow was blocked by simply applying external pressure and restored back by releasing the pressure. The fabricated FMGC outfitted with the FCD is shown in Fig. 1.

To conduct the FMGC-based sandwich and competition immunoassays, CTX-II antibodies and PEG_4-EKGPDP were immobilized on the sensing areas of the FMGC. Then, the prepared CTX-II samples based on real urine and artificial serum sample were applied with CTX-II antibody-conjugated fluoro-microbeads. The numbers of surface-bound optical probes were counted for quantification of CTX-II analysis. In this study, we simultaneously analyzed sCTX-II and uCTX-II accurately and rapidly by using the FMGC-based assay, covering the required clinical detection range for osteoarthritis. The validity of the developed assay was checked by conducting tests in a similar format by using a conventional ELISA kit and comparing the results, indicating that the developed FMGC-based assays could be successfully utilized for the CTX-II analyses. Details are reported herein.

2. Experimental procedures

2.1. Chemicals and apparatus

FluoSpheres carboxylate-modified microspheres (excitation/emission wavelengths=540/560 nm, diameter=200 nm) were from Molecular Probes. Human albumin protein was purchased from Fitzgerald. The urine samples were acquired from Bio-Rad (human, product number Q-1513). Main ingredients are creatinine, urea, uric acid, glucose and inorganic molecules (calcium, phosphorus, potassium, and magnesium) as well as antibodies. The CTX-II antibody was purified by Abclone Ltd. The EKGPDP and PEG_4-EKGPDP peptides were obtained from Peptron Inc. The conventional ELISA kits were from IDS and Elabscience. 3.3′-Dithiobis(sulfosuccinimidylpropionate) (DTSSP) was acquired from Thermo Scientific. The 200 mM HEPES (pH 7.4), PBST-I (50 mM PBS, 150 mM NaCl, and 0.1% Triton X-100, pH 7.4), PBST-II (PBST containing 0.1% BSA, pH 7.4) were used. The artificial serum solution was produced in 200 mM HEPES buffer and contained 0.1% human albumin protein, 2.5 mM urea, 4.7 mM D-(+)-glucose, 5 mM $CaCl_2$, 4.5 mM KCl, 145 mM NaCl, and 1.6 mM

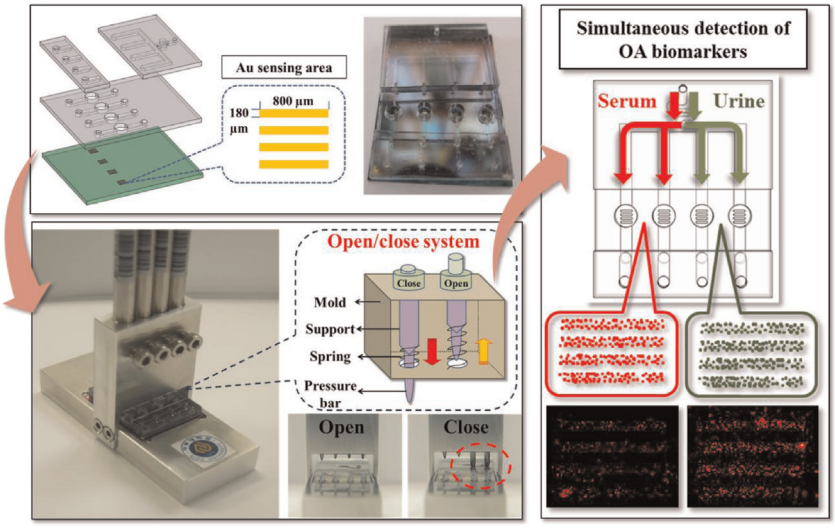

Fig. 1. Schematic diagram of the CTX-II immunosensing system. The developed fluoro-microbeads guiding chip (FMGC) is controlled by a fluidic control device (FCD), allowing for the simultaneous detection of urinary and serum CTX-II.

Please cite this article as: Park, Y.M., et al., Biosensors and Bioelectronics (2014), http://dx.doi.org/10.1016/j.bios.2014.08.016

$MgCl_2$ (Sezginturk, 2011). The concentration of urinary creatinine was analyzed by using the Reflotron Plus system (Roche). Fluorescence images were visualized using a fluorescence microscope (Leica DM 4000B) and were analyzed using Image J software (NIH).

2.2. Conjugation of CTX-II antibody to fluoro-microbeads

To covalently couple the CTX-II antibodies to the carboxylate-modified microbeads, the carboxylate groups were activated using water-soluble EDC and NHS. First, 20 μL of 5 mM EDC and 20 μL of 8 mM sulfo-NHS were added to 400 μL of 0.1% carboxylate-modified beads diluted in MES buffer and the mixture was incubated for 15 min at the room temperature. To form amide bonds between the fluoro-beads and antibodies, 100 μL of 50 μg/mL uCTX-II antibody was incubated with the beads for 2 h at room temperature. Next, 20 μL of 1 M L-lysine in 0.008% PEG solution was added to minimize nonspecific binding to the microbeads by blocking the activated carboxyl group and hydrophobic site on their surfaces. The antibody-conjugated fluoro-microbeads were diluted in PBST-II. The optical probes diluted to 0.0007% and 0.007% (v/v) were used to analyze sCTX-II and uCTX-II, respectively.

2.3. Fabrication of the FMGC

To fabricate the gold-patterned substrate of the FMGC, Ti/Au (500/2000 Å) was deposited and patterned on a thermally oxidized silicon wafer by sputtering. The designed gold pattern size on the substrate was $180 \times 800\ \mu m^2$. The middle and top channel layers made of PDMS were fabricated using a soft-lithography technique. The PDMS prepolymer (1:10 base polymer to curing agent) was poured onto patterned SU-8 masters that were created by a lithography process using SU-8 (SU-8 2100, MicroChem) negative thick photoresist on a thermally oxidized silicon wafer. The thicknesses of the middle and top channels were 110 μm. After curing at 65 °C for 1 h in a vacuum oven, the PDMS replicas were peeled off the masters. The holes of the PDMS channels were punched out and then the top and middle PDMS layers were bonded by corona plasma using a handmade plasma jet system. Fig. 2 shows a photograph of the fabricated FMGC with dimensions of $20 \times 30 \times 3.5\ mm^3$.

2.4. uCTX-II and sCTX-II sample preparation

To detect CTX-II in the urine and serum, various concentrations of uCTX-II and sCTX-II solutions were prepared. The urine samples were spiked with purified EKGPDP peptide at concentrations ranging from 200, 350, 700, 1400 and 2800 ng/mmol (corrected value *vs.* creatinine). Because the biomarkers in human urine are usually expressed as a ratio to the urinary creatinine concentration, the concentration of the prepared uCTX-II was corrected using the following formula (1) (Waikar et al., 2010; Tonomura et al., 2013):

$$\begin{aligned} &Corrected\,CTX-II\,value\,(\mathrm{ng/mmol}) \\ &= \frac{1000 \times CTX-II\,conc.\,from\,ELISA\,(\mathrm{ng/mL})}{Conc.\,from\,Creatinine\,(\mathrm{mmol/L})} \end{aligned} \quad (1)$$

To prepare the sCTX-II sample solutions, the standard reagents from a human sCTX-II ELISA kit were dissolved in artificial serum solutions ranging in concentration from 0, 0.1, 0.2, 0.5, 1.0, 2.0 and 2.5 ng/mL. The prepared urine and serum samples were analyzed using conventional ELISA to verify the accuracy of their concentrations and were applied to the FMGC assay without dilution. This study was approved by the Institutional Review Board (IRB, 201309-HM-EX-001) at Ajou University.

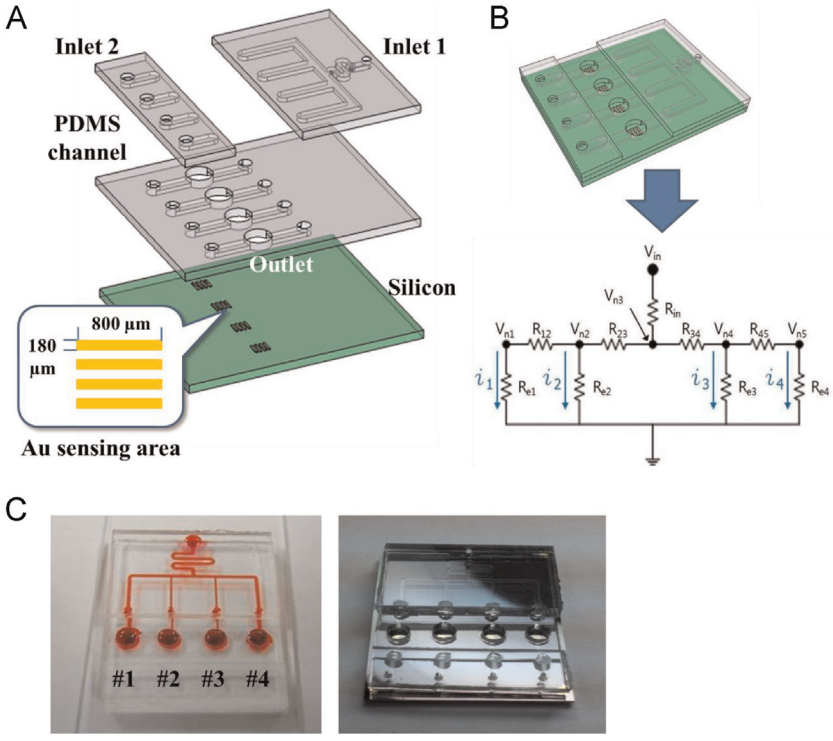

Fig. 2. Schematic illustration of the fluoro-microbeads guiding chip (FMGC). (A) The designed FMGC has three layers. The bottom layer includes $180 \times 800\ \mu m^2$ Au sensing areas on a silicon substrate. The middle and top channel layers are composed of polydimethylsiloxane (PDMS). The middle channel layer has four sensing areas that are connected to the top channel layer *via* holes. The top channel layer includes one injection inlet (inlet 1) and four injection inlets (inlet 2). (B) An electrical model of the microfluidic channel of a sample inlet, where *V* is the voltage, *i* is the current, and *R* is the resistances of each channel structure. (C) The resistance-balanced channels were fabricated in glass, and flow transfer was tested by injecting red ink (left). The fabricated FMGC modified with the gold pattern sensing areas (right).

Please cite this article as: Park, Y.M., et al., Biosensors and Bioelectronics (2014), http://dx.doi.org/10.1016/j.bios.2014.08.016

2.5. Manipulation of the FMGC surface for uCTX-II and sCTX-II analysis

To analyze the uCTX-II, we employed a competition-type immunoassay. Before assay on FMGC, the PBST-I solution was applied (5 min) to the PDMS channel in order to make the surface hydrophilic. PEG_4-EKGPDP, an uCTX-II analog PEGylated hexapeptide, was immobilized on the sensing area of the FMGC by using a self-assembled monolayer (SAM) technique. Through inlet 1, 5 mM DTSSP in double-distilled and deionized water (DDW) was loaded and reacted for 2 h. The FMGC surfaces were then washed with DDW. PEG_4-EKGPDP, dissolved to 1 mM in 0.1 M PBS, was injected into inlet 1. To remove the unreacted succinimidyl groups of the DTSSP, 10 mM ethanolamine in 0.1 M bicarbonate buffer (pH 9.4) was added for 30 min. After rinsing with PBS, PBST-II solution was incubated with the FMGC surfaces for 30 min to prevent non-specific binding. The chips were stored in PBS at 4 °C until use.

To perform the sandwich-type immunoassay for the detection of sCTX-II, CTX-II antibodies were immobilized on the FMGC sensing areas by using the procedure outlined above. Into the inlet 1, 30 μL of 5 mM DTSSP solution was loaded and reacted for 2 h. After washing with DDW, 30 μL of 100 μg/mL CTX-II antibody was applied through inlet 1 for 1 h. The remaining succinimidyl groups were blocked by injecting 10 mM ethanolamine solution for 30 min. Prepared PBST-II solution was applied for 30 min. The FMGCs were stored at 4 °C when not in use.

2.6. Immunoassay analysis of urinary and serum CTX-II

To assess uCTX-II by using the competition-type immunoassay, various concentrations of urine samples were pre-mixed with 0.007% (v/v) optical probe at a volume ratio of 1:1 for 1 h at room temperature. The pre-mixed solutions were individually applied for 10 min to the sensing areas which were coated with PEG_4-EKGPDP through inlet 2. After biospecific recognition, the unbound optical probe was washed out by injecting PBST-I and PBST-II solutions into inlet 1. The remaining solution in the FMGC channel was completely removed. To observe the optical signal, fluorescence microscopy was employed by using a green filter that matched the excitation wavelength of the beads (excitation/emission maxima = 540/560 nm). From the resulting images, the numbers of beads were quantified using the Image J software. To obtain the specificity of the immunoassay signal, we compared the signals from patterns outside and inside the FMGC sensing area.

For the sandwich-type immunosensing, the prepared sCTX-II was reacted with the antibody-modified sensing area at room temperature for 20 min. After washing with PBS, the optical probe at a concentration of 0.0007% (v/v) was applied for 10 min. The sensing area was then rinsed with PBST-I and PBST-II. The optical signals were measured as described above.

2.7. Simultaneous detection of urinary and serum CTX-II

To simultaneously detect urinary and serum CTX-II on a single FMGC, PEG_4-EGKPDP and CTX-II antibodies were immobilized on the sensing areas by using the amine-reactive SAM method. To inlet 1, 30 μL of 5 mM DTSSP diluted in DDW was applied over the course of 2 h. After washing with DDW, 10 μL of 1 mM PEG_4-EKGPDP and 100 μg/mL CTX-II antibodies were applied to sensing areas #1 and #3, respectively, for 1 h. PBS solution was loaded into sensing areas #2 and #4 as a negative control. (The channel numbers are shown in Fig. 2(C), *vide infra*). After washing with PBS, each sensing area was blocked using ethanolamine and BSA. The low (0.5 ng/mL sCTX-II and 200 ng/mmol uCTX-II), moderate (1.0 ng/mL sCTX-II and 350 ng/mmol uCTX-II), and high (2.0 ng/mL sCTX-II and 700 ng/mmol uCTX-II) concentration samples were simultaneously applied and analyzed. The serum samples were loaded into channel #3 and #4 for 20 min while channels #1 and #2 were blocked by FCD. The 0.0007% (v/v) optical probe was then applied to channels #3 and #4 for 10 min. Next, the urine samples that had been premixed with 0.007% (v/v) optical probe for 1 h was immediately applied for 10 min to channels #1 and #2, while channel #3 and #4 were blocked. Upon completion of the assay, the FMGC was washed with PBST-I and PBST-II sequentially, and the optical signal was observed using a fluorescence microscope as described above.

3. Results and discussion

3.1. Manipulation of the fluoro-microbeads guiding chip

To simultaneously analyze the OA biomarkers present in various samples, we designed and fabricated an immunosensing chip possessing the signaling capability based on fluoro-microbeads counting (on FMGC). The fabricated FMGC is composed of three layers laminated (Fig. 2(A)). The bottom layer included a $180 \times 800\ \mu m^2$ gold pattern on a silicon substrate for optical sensing. The middle channel layer had four sensing areas that were connected to the top channel layer through inter-connecting holes. The top channel layer included one sample injection inlet (inlet 1) and four injection inlets (inlet 2). In the FMGC channel layer, the passing time of the fluids from inlet 1 to each sensing area differed during the sample injection process. It is for the reason that the fluidic resistance differed between each channel in the FMGC for proper fluidic operation. Therefore, the sample volumes in the central channels were larger than the outer channels because the outside channels were longer than central channels. To balance these volumes, structural changes to the channels used in the sample injection process are required to ensure an accurate sensing process. In hydraulic systems, the pressure-related microfluidic network is usually analyzed using analog electric systems (Kim et al., 2006; Oh et al., 2012). Fig. 2(B) shows an electrical model of the microfluidic channel for the sample inlet, where V is the voltage, i is the current, and R is the resistance of each channel structure. When a steady voltage was applied, the node voltages of V_{n1} and V_{n2} were different. Therefore, the currents passing the resistances in the microfluidic channels are different, causing inconsistent flow rates of the samples in each channel. To adjust the balance of the sample volume, we must modify the resistance between the channels by changing their size. Based on the channel structure, the formula for the calculation of the hydraulic resistance was derived. In this study, the FMGC channel was rectangular, and the hydraulic resistance R was calculated according to Eq. (2) (Brivio et al., 2005).

$$R = \frac{4\mu l}{ab^3}\left\{\frac{16}{3} - 3.36\frac{b}{a}\left(1 - \frac{b^4}{12a^4}\right)\right\}^{-1} \quad (2)$$

where a and b are the half width and height of the microfluidic channel, μ is the fluid viscosity, and the l is the channel length. To adjust the channels so that they had the same hydraulic resistances, we modified the channel width. As shown in Fig. 2(B), the total resistance of R_{12} and R_{e1} must be equal to the R_{e2} to obtain same currents for i_1 and i_2. Thus, the channel width of R_{12} and R_{e1} should be half of that of R_{e2} according to Eq. (2). Based on this analysis, the channel widths of R_{e2} and R_{e3} should be 0.25 mm, while the channel widths of R_{e1} and R_{e4} should be 0.5 mm. The lengths of the vertical channels were fixed at 5 mm.

To evaluate the flow in the modified channels, a finite element model analysis, using the FEMLAB software package, was used to perform a simulation test. The working fluid was DDW, and the

Please cite this article as: Park, Y.M., et al., Biosensors and Bioelectronics (2014), http://dx.doi.org/10.1016/j.bios.2014.08.016

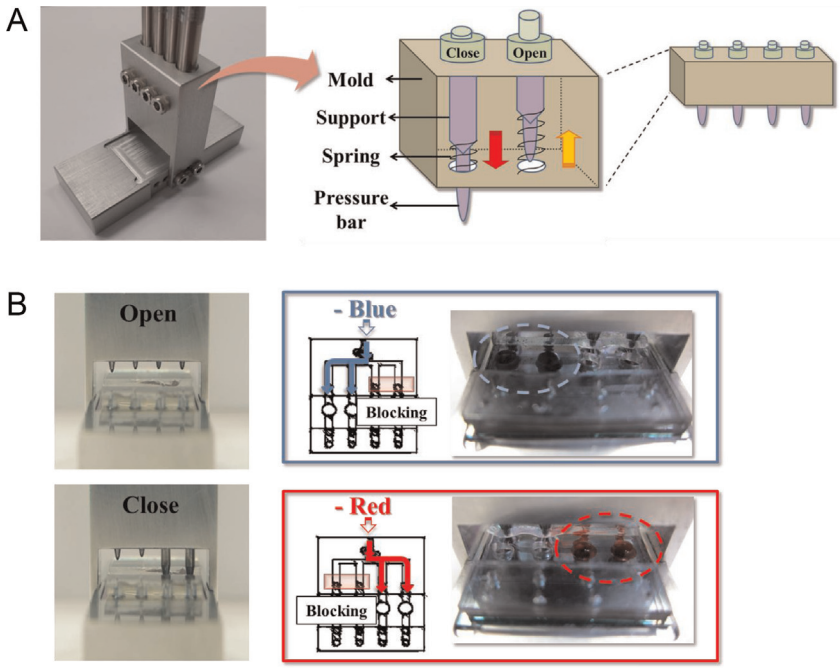

Fig. 3. (A) Manipulation of the fluidic control device (FCD). The mold was fabricated using a computer numerical control (CNC) machining technique. The FCD consists of a pressure bar, spring, support, and open–close button. (B) FMGC channels partially blocked using the FCD were tested by injecting blue (upper) and red (lower) dyes.

pressure at the inlet 1 was 100 Pa. To verify the flow rate, we calculated the velocity of each channel based on the simulation results. The volumetric flow rates of the inner and outer simple channels were 0.30×10^{-12} m^3/s and 0.15×10^{-12} m^3/s, respectively, while the flow rates of the resistance-balanced channels were 0.18×10^{-12} m^3/s. Based on these consideration, the resistance-balanced channels were fabricated on the glass surface and we tested the flow transfer by injecting red ink. The same volume of sample was successfully moved along each channel. Based on the results, we fabricated the FMGC as shown in Fig. 2(C). The channel numbers were assigned from left to right.

3.2. Application of the fluidic control device

To simultaneously detect CTX-II in serum and urine on a single chip, the FMGC channels must be individually controlled because the sample injection hole at inlet 1 is contiguous with all the sensing channels. To achieve this function in the immunosensing system, we designed and employed a FCD as shown in Fig. 3.

To control the sample flow in FMGC channel, we attempted to block the middle of the channel layer. The FMGC channel was fabricated from PDMS, which possess a high elasticity. By exploiting this property, the PDMS channels could be easily blocked by external pressure, while maintaining the channel structure around the opening. PDMS also quickly returns to its original form after the release of the pressure. Therefore, we installed a small pressure bar onto the upper part of the FCD (Fig. 3(A)). The mold was fabricated using a computer numerical control (CNC) machining technique, and the four pressure bars were installed, one for each FMGC channel. To reversibly compress the PDMS channels, a spring and push-pull button was added. In this study, a mini push-pull ballpoint pen was modified and used as a pressure apparatus. The upper mold was fabricated to move front to back in order to effectively match the mold location with the FMGC channel. The bottom mold functions to affix the upper mold, including the FMGC location area.

Using the fabricated FCD, we were able to simply and separately control the open/close system of the FMGC channels. To confirm the utility of the FCD, we tested the flow by loading red and blue ink into the fabricated system. As shown in Fig. 3(B), we injected the ink into the FMGC channels, while two of four channels were blocked using the FCD. The ink traveled along the open channels, while the ink was unable to pass through the closed channels. The results clearly demonstrated that the fluid in the channels could be controlled individually. Thus, the developed FCD is sufficient for the controlled movement of samples and the simultaneous detection of CTX-II in urine and serum on a single FMGC.

3.3. Urinary CTX-II analysis employing competitive immunoassay

Urinary CTX-II may include the EKGPDP epitope or monomeric epitope variants. Because of the unique structural properties of uCTX-II, a competition-type immunoassay was conducted on the FMGC. PEG_4-EKGPDP, an uCTX-II analog, was immobilized on the FMGC sensing area. CTX-II antibody, which specifically recognizes the EKGPDP peptide, was mixed with target uCTX-II in real urine sample and was then applied to the PEG_4-EKGPDP-modified sensing area. To observe the optical signal from affinity assay, the CTX-II antibody was conjugated to fluoro-microbeads.

In healthy humans, the concentration of uCTX-II in urine is typically below 400 ng/mmol, thus this was used as a cut-off value for signaling (Garnero et al., 2002, 2003). We detected uCTX-II at concentrations ranging from 200–2800 ng/mmol, which spanned the cut-off value covering the clinical requirements for OA diagnosis. Each uCTX-II sample was applied to a separate FMGC sensing area. The competition assay results are shown in Fig. 4(A).

The optical probes used in the FMGC tests were predominantly detected inside the sensing pattern, while only a few optical probes were observed outside the pattern (Fig. 4, inset). These data indicated that minimal non-specific binding occurred between the biomolecules in the urine and the optical probes in the prepared sensing area. uCTX-II was quantitatively analyzed by counting the number of beads on the FMGC sensing area in the images by using Image J software. The specificity of the optical signal was assessed by comparing the signal from inside

Please cite this article as: Park, Y.M., et al., Biosensors and Bioelectronics (2014), http://dx.doi.org/10.1016/j.bios.2014.08.016

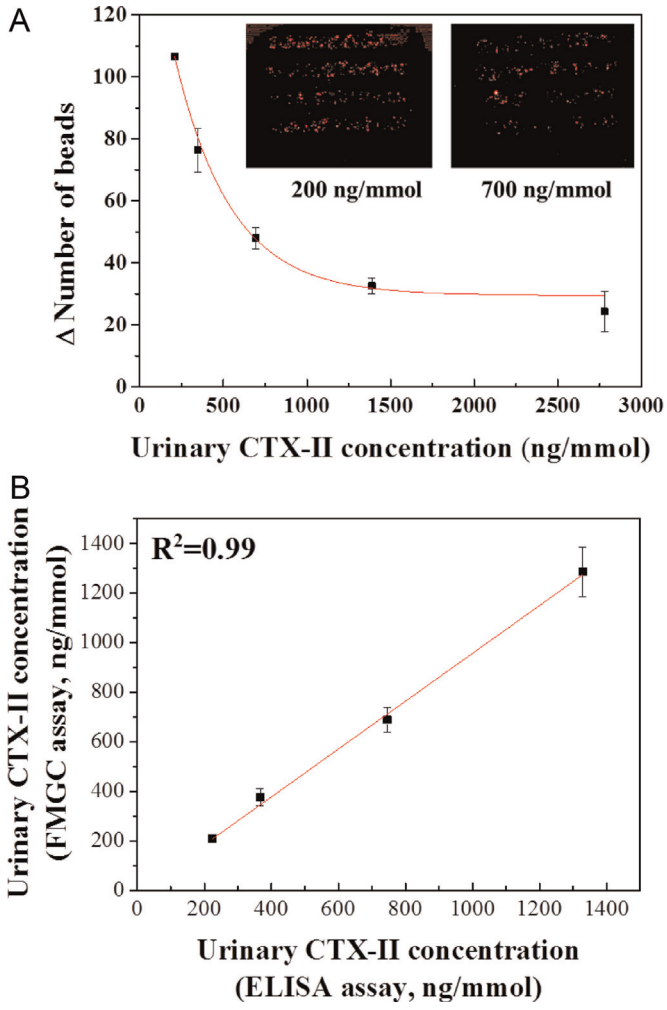

Fig. 4. (A) Calibration curve for the urinary CTX-II (uCTX-II) competition assay. uCTX-II at concentrations ranging from 200–2800 ng/mmol in real urine sample was quantitatively analyzed. The assay was conducted three times and the error bars indicate the standard deviations. The images obtained from the FMGC assay at different uCTX-II concentrations are shown in the inset. (B) Correlation between the FMGC-based competition assay and a commercially available uCTX-II enzyme-linked immunosorbent assay (ELISA). uCTX-II concentrations from 200–1400 ng/mmol are plotted. The assay was performed three times and the error bars indicate the standard deviations.

($180 \times 800\ \mu m^2$) and outside of the pattern in the result image. We found that the optical signal was inversely proportional to the concentration of uCTX-II in the range of 200–1400 ng/mmol. The calibration curve based on the assay results is shown in Fig. 4(A). Considering the cut-off value of uCTX-II is 400 ng/mmol, the calibration curve we obtained could feasibly distinguish the uCTX-II levels in OA patients *vs.* healthy humans. Although the obtained calibration curve was saturated at uCTX-II concentrations above 1400 ng/mmol, this assay fulfills the clinically required detection range because uCTX-II concentration in osteoarthritis patients is usually below 1000 ng/mmol.

To evaluate the accuracy of the FMGC-based assay, these results were compared with those obtained using a conventional uCTX-II ELISA kit. The uCTX-II samples used in the competition-type assay were measured using an ELISA kit. Because the signals leveled off at concentrations above 1400 ng/mmol, the results of the FMGC-based assay and ELISA were compared for uCTX-II concentrations ranging from 200–1400 ng/mmol. The results of the ELISA and FMGC-based assay were highly correlated (R^2 value of 0.99; Fig. 4 (B)). The slope of the calibration curve was 0.98, indicating that the competition assay developed for uCTX-II analysis was highly accurate. To assess the variation of the assay, the same uCTX-II samples were assayed at least three times. The coefficients of variation of the obtained optical signals were approximately 9%, indicating that the developed assay was suitable for OA diagnosis. The limit of detection (LOD), which was calculated as three times the standard deviation of the background signal, was 50 ng/mmol for the FMGC-based assay. This LOD was similar to that of the commercial ELISA (30 ng/mmol). Notably, an accurate analysis of uCTX-II was completed within 70 min, while the ELISA required more than 20 h to obtain the final results. Based on this result, we achieved accurate and reliable assay results using real urine samples, and the detection could be executed rapidly.

3.4. Serum CTX-II analysis employing sandwich immunoassay

In this study, we also analyzed serum CTX-II to accurately assess the OA. As mentioned previously, the sCTX-II may contain the cross-linked homo-dimeric epitope (EKGPDP). Based on this structural property, we could employ a sandwich-type immunoassay using a single antibody to detect sCTX-II.

In healthy humans, the concentration of sCTX-II is below 1 ng/mL, which was used as the cut-off value (Tang et al., 2012). Thus, we performed the sandwich assay by using sCTX-II concentrations ranging from 0.1–2.5 ng/mL in artificial serum sample, which spanned the cut-off value and covered the clinical requirements for OA assessment. The prepared sCTX-II samples were assayed using the FMGC. The calibration curve obtained from the sandwich assay results (Fig. 5(A)) and the corresponding images (Fig. 5(A), inset)) of the FMGC sensing areas are presented.

As shown in the calibration curve, all the sCTX-II samples were found to be proportional to the sCTX-II concentration and the optical signal leveled off at 2.0 ng/mL. In accordance with the results of the uCTX-II assay, the FMGC assay developed for sCTX-II was able to distinguish the sCTX-II levels of patients from those of healthy subjects. The LOD calculated in the linear detection range of 0.1–2.0 ng/mL was approximately 0.1 ng/mL. This LOD value was comparable to that of the commercial ELISA (0.1 ng/mL). Thus, these results assay demonstrated that the proposed assay had reasonable performance in comparison to the ELISA.

To confirm its efficiency, we compared the results obtained using the FMGC-based assay and the ELISA. The linear detection range (0.1–2.0 ng/mL) was compared, and the same sample was used in each assay. The result from sCTX-II assay is shown in Fig. 5 (B). The registered slopes was 0.98 (R^2=0.97), demonstrating a high correlation between two assays. To assess the variation of the sandwich-type immunoassay, FMGC assay was performed multiple times using the same sCTX-II samples under same assay conditions (duration, temperature, and pH). The calculated coefficients of variation were approximately 12%, supporting that the developed assay could be used for OA diagnosis. Taken together, our data demonstrated that the FMGC-based assay for sCTX-II analysis based on the artificial serum is reliable for OA diagnosis, and this assay could be feasibly used in the diagnostic field in place of ELISA.

3.5. Multiple sensing of urinary and serum CTX-II

In the previous sections, CTX-II in the urine and serum was analyzed separately. In addition to this, the multiple sensing of the OA biomarkers is helpful to achieve accurate OA diagnoses. Therefore, we aimed to simultaneously detect CTX-II in urine and serum on a single chip. As shown in Fig. 2(C), the FMGC contained four

Please cite this article as: Park, Y.M., et al., Biosensors and Bioelectronics (2014), http://dx.doi.org/10.1016/j.bios.2014.08.016

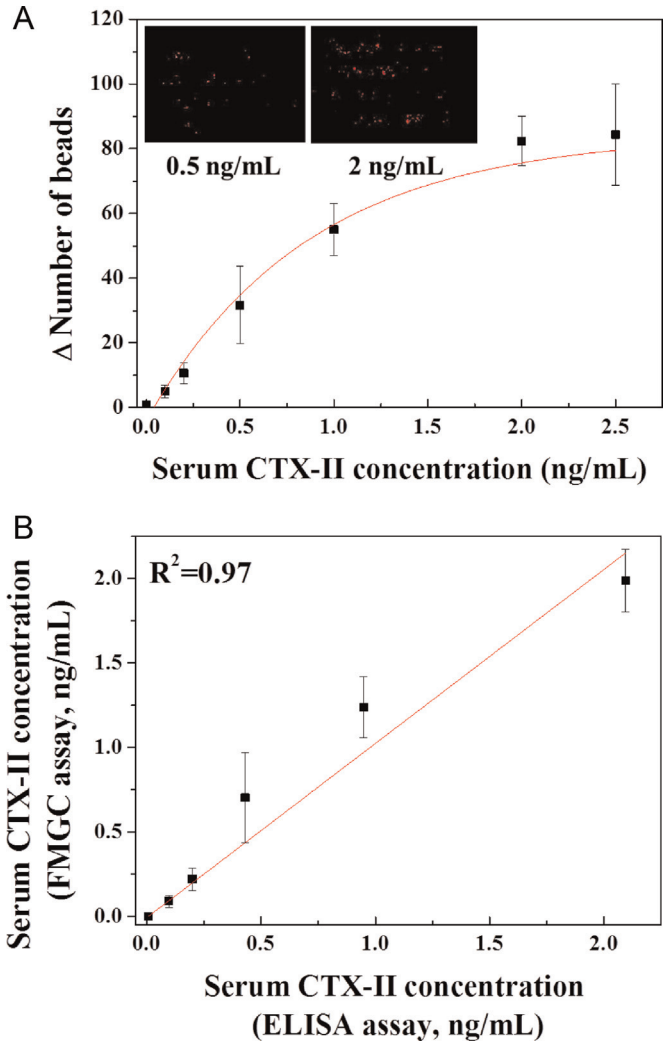

Fig. 5. (A) Quantitative analysis of serum CTX-II (sCTX-II) by using a sandwich assay. sCTX-II concentrations ranging from 0–2.5 ng/mL in artificial serum sample were quantitatively tested. The average of assays performed in triplicate is shown with error bars indicating the standard deviations. The inset shows the registered optical image obtained from the FMGC assay at different sCTX-II concentrations. (B) Correlation analysis between the FMGC-based sandwich assay and a standard ELISA that detects sCTX-II. sCTX-II concentrations ranging from 0–2 ng/mL are presented. The assay was performed in triplicate and the error bars indicate the standard deviations.

separate sensing areas. The corresponding channels were numbered from left to right.

Sensing areas #1 and #3 were modified with PEG_4-EKGPDP and CTX-II antibodies, respectively, as a positive control for the uCTX-II and sCTX-II analysis. Sensing areas #2 and #4 were blocked using ethanolamine and BSA as a negative control. Using a prepared FMGC, low (200 ng/mmol of uCTX-II and 0.5 ng/mL of sCTX-II), moderate (350 ng/mmol of uCTX-II and 1.0 ng/mL sCTX-II), and high (700 ng/mmol of uCTX-II and 2.0 ng/mL sCTX-II) CTX-II concentrations were applied, spanning the cut-off values. Each concentration was simultaneously assayed on a single chip. While the urine samples loaded along channels #1 and #2, channels #3 and #4 were blocked using the FCD as shown in Fig. 3(C). The serum samples were then applied to channels #3 and #4, while blocking channels #1 and #2 by using the FCD. The test results of the ELISA and FMGC assays for uCTX-II and sCTX-II are presented in Table 1.

The results indicated that the multiple sensing was achieved as intended, allowing high response with each calibration curve. We

Table 1
Multiple sensing of urinary and serum CTX-II. The urinary (200, 400, and 700 ng/mmol) and serum CTX-II (0.5, 1.0, and 2.0 ng/mL) were simultaneously assayed. The test results of the ELISA and FMGC assays for urinary and serum CTX-II are presented. The signal recovery of FMGC assay compared to the ELISA is also presented. Average recovery is 103 ± 10%.

Sample and assay type	FMGC test	ELISA test	Signal recovery to ELISA (%)
uCTX-II (ng/mmol) (Competition assay)	215 ± 2	208 ± 4	103 ± 1
	340 ± 18	346 ± 15	98 ± 5
	671 ± 48	693 ± 13	97 ± 6
sCTX-II (ng/mL) (Sandwich assay)	0.5 ± 0.1	0.4 ± 0.1	109 ± 23
	1.1 ± 0.1	1.0 ± 0.1	106 ± 10
	2.1 ± 0.4	2.0 ± 0.2	105 ± 19

calculated the signal recovery of the FMGC assay to that of conventional ELISA by using the following Eq. (3):

$$Recovery = \frac{CTX - II\,conc.\ from\ developed\ assay}{CTX - II\,conc.\ from\ ELISA} \times 100(\%) \quad (3)$$

The signal recovery was calculated to be 103 ± 10% (average value from Table 1), supporting that the two assays were highly correlated. To investigate the intra-assay variation, the assay was performed multiple times using the same antigen samples and experimental conditions. The coefficient of variation value was approximately 10%, demonstrating that the multiple assay developed for CTX-II detection in urine and serum is reliable.

In summary, the FMGC-based CTX-II detection assay was simpler than commercial ELISA because the optical probes directly generate the optical signal, whereas ELISA require extra time for the enzyme and substrate to react. We achieved an accurate analysis of both urinary and serum CTX-II within approximately 1 h by using FMGC. In contrast, conventional CTX-II ELISA require 3.5 h for sCTX-II and a full day for uCTX-II analysis. Only 30 μL of solution was need to fill each sensing channel from inlet 1 of the FMGC and 10 μL of sample solution was required for a single assay when using the FMGC at inlet 2, reducing the burden of patients undergoing OA diagnosis. In contrast, a conventional ELISA consumes several dozen of microliters for the completion of one assay. Also, we achieved the reliable analysis for CTX-II based on real urine and artificial serum. The purpose of this study was to diagnose OA by quantitatively analyzing OA biomarkers on a single chip. Our results suggest that the developed FMGC-based assay is suitable for CTX-II analysis in clinical research.

4. Conclusions

In this study, we attempted to establish an accurate and rapid biosensing strategy for CTX-II, both for the urine and serum specimens, as a diagnostic tool for osteoarthritis. The proposed FMGC-based competition and sandwich assays accurately detected CTX-II, and the results obtained using this assay correlated well with those obtained using commercial ELISA kits. In addition, we demonstrated that the FMGC-based multiple analysis system, when used in conjunction with the FCD, effectively and quantitatively assessed urinary and serum CTX-II simultaneously. A notable advantage of the developed system was the simple control of the microfluidics. This simplicity allows for numerous osteoarthritis biomarkers in various body fluids to be simultaneously applied and analyzed. Therefore, we suggest that FMGC and FCD-based multiple-sensing system would be a promising tool that can be used for osteoarthritis diagnosis.

Please cite this article as: Park, Y.M., et al., Biosensors and Bioelectronics (2014), http://dx.doi.org/10.1016/j.bios.2014.08.016

ARTICLE IN PRESS

Acknowledgments

This study was supported by Korea Ministry for Health, Welfare, and Family Affairs (A091120), Priority Research Centers Program (2009-0093826) and National Research Foundation of Korea (NRF-2013R1A1A2A10058404).

References

Bauer, D.C., Hunter, D.J., Abramson, S.B., Attur, M., Corr, M., Felson, D., Heinegård, D., Jordan, J.M., Kepler, T.B., Lane, N.E., Saxne, T., Tyree, B., Kraus, V.B., 2006. Osteoarthr. Cartil. 14, 723–727.
Birmingham, J.D., Vilim, V., Kraus, V.B., 2006. Biomark. Insights 1, 61–76.
Brivio, M., Tas, N.R., Goedbloed, M.H., Gardeniers, H.J., Verboom, W., van den Berg, A., Reinhoudt, D.N., 2005. Lab Chip 5, 378–381.
Ding, C., Garnero, P., Cicuttini, F., Scott, F., Cooley, H., Jones, G., 2005. Osteoarthr. Cartil. 13, 198–205.
Elsaid, K.A., Chichester, C.O., 2006. Clin. Chim. Acta 365, 68–77.
Eyre, D.R., Weis, M.A., Wu, J.-J., 2008. Methods 45, 65–74.
Garnero, P., 2007. BoneKEy – Osteovision 4, 7–18.
Garnero, P., Ayral, X., Rousseau, J.C., Christgau, S., Sandell, L.J., Dougados, M., Delmas, P.D., 2002. Arthritis Rheum. 46, 2613–2624.
Garnero, P., Conrozier, T., Christgau, S., Mathieu, P., Delmas, P.D., Vignon, E., 2003. Ann. Rheum. Dis. 62, 939–943.
Giljohann, D.A., Mirkin, C.A., 2009. Nature 462, 461–464.
Hanash, S.M., Pitteri, S.J., Faca, V.M., 2008. Nature 452, 571–579.
Hong, S.Y., Park, Y.M., Jang, Y.H., Min, B.-H., Yoon, H.C., 2012. BioChip J. 6, 213–220.
Kim, D., Chesler, N.C., Beebe, D.J., 2006. Lab Chip 6, 639–644.
Kim, S.J., Park, Y.M., Min, B.-H., Lee, D.S., Yoon, H.C., 2013. Biochip J. 7, 399–407.
Kong, S.Y., Stabler, T.V., Criscione, L.G., Elliott, A.L., Jordan, J.M., Kraus, V.B., 2006. Arthritis Rheum. 54, 2496–2504.
Kraus, V.B., Burnett, B., Coindreau, J., Cottrell, S., Eyre, D., Gendreau, M., Gardiner, J., Garnero, P., Hardin, J., Henrotin, Y., Heinegård, D., Ko, A., Lohmander, L.S., Matthews, G., Menetski, J., Moskowitz, R., Persiani, S., Poole, A.R., Rousseau, J.C., Todman, M., OARSI, F.D.A., 2011. Osteoarthr. Cartil. 19, 515–542.
Lohmander, L.S., 1997. Baillieres Clin. Rheumatol. 11, 711–726.
Lohmander, L.S., Atley, L.M., Pietka, T.A., Eyre, D.R., 2003. Arthritis Rheum. 48, 3130–3139.
Lotz, M., Martel-Pelletier, J., Christiansen, C., Brandi, M.-L., Bruyère, O., Chapurlat, R., Collette, J., Cooper, C.h., Giacovelli, G., Kanis, J.A., Karsdal, M.A., Kraus, V., Lems, W.F., Meulenbelt, I., Pelletier, J.-P., Raynauld, J.-P., Reiter-Niesert, S., Rizzoli, R., Sandell, L.J., Van Spil, W.E., Reginster, J.-Y., 2013. Ann. Rheum. Dis. 72, 1756–1763.
Oh, K.W., Lee, K., Ahn, B., Furlani, E.P., 2012. Lab Chip 12, 515–545.
Park, Y.M., Kim, S.J., Kim, K., Han, Y.D., Yang, S.S., Yoon, H.C., 2013. Sens. Actuators B: Chem. 186, 571–579.
Roos, H., Adalberth, T., Dahlberg, L., Lohmander, L.S., 1995. Osteoarthr. Cartil. 3, 261–267.
Rousseau, J.C., Delmas, P.D., 2007. Nat. Clin. Pract. Rheumatol. 3, 346–356.
Sezginturk, M.K., 2011. Biosens. Bioelectron. 26, 4032–4039.
Song, S.Y., Han, Y.D., Hong, S.Y., Kim, K., Yang, S.S., Min, B.-H., Yoon, H.C., 2012. Anal. Biochem. 420, 139–146.
Song, S.Y., Han, Y.D., Kim, K., Yang, S.S., Yoon, H.C., 2011. Biosens. Bioelectron. 26, 3818–3824.
Tang, X., Zhou, Z., Shen, B., Yang, J., Kang, P., Li, J., Crook, N., Li, Q., Min, L., Pei, F., 2012. Rheumatol. Int. 32, 3503–3509.
Tonomura, Y., Morikawa, Y., Takagi, S., Torii, M., Matsubara, M., 2013. Toxicology 303, 169–176.
Waikar, S.S., Sabbisetti, V.S., Bonventre, J.V., 2010. Kidney Int. 78, 486–494.
Wildi, L.M., Tamborrini, G., 2011. In: Martel-Pelletier, J., Pelletier, J.-P. (Eds.), Understanding Osteoarthritis from Bench to Bedside. Research Signpost, India, pp. 103–125.
Zhang, Y., Jordan, J.M., 2010. Clin. Geriatr. Med. 26, 355–369.

Please cite this article as: Park, Y.M., et al., Biosensors and Bioelectronics (2014), http://dx.doi.org/10.1016/j.bios.2014.08.016